Adsorption Equilibrium, Kinetics, and Enthalpy of N_2O on Zeolite 4A and 13X

Dipendu Saha* and Shuguang Deng

Chemical Engineering Department, New Mexico State University, Las Cruces, New Mexico 88003

The adsorption equilibrium, kinetics, and enthalpy of nitrous oxide adsorption on zeolites 4A and 13X were measured volumetrically at temperatures of (194, 237, and 298) K and gas pressure up to 108 kPa. It was found that zeolite 4A adsorbs more N_2O than 13X in all of the conditions used. The Langmuir, Freundlich, and Toth isotherm models were employed to correlate the adsorption isotherms. N_2O diffusivity in these adsorbents at 298 K was calculated from the adsorption kinetic uptake curves by using a simple micropore diffusion model. It was found that the average diffusivity values in zeolite 4A and 13X are ($3.38 \cdot 10^{-14}$ and $1.05 \cdot 10^{-12}$) $m^2 \cdot s^{-1}$, respectively. The heat of adsorption values are between (−33 and −21) $kJ \cdot mol^{-1}$ for zeolite 4A and (−28 and −22) $kJ \cdot mol^{-1}$ for 13X for adsorption loadings between (0.5 and 3.5) $mmol \cdot g^{-1}$.

1. Introduction

Nitrous oxide (N_2O) is one of the major industrial byproduct gases that is generated from industrial synthesis facilities for producing nitric acid, adiptic acid, or nylon.[1,2] It is identified as a very acute greenhouse gas that is 150 times stronger than that of carbon dioxide.[3,4] Besides having the greenhouse gas properties, it can also deplete the ozone layer, thereby making it one of the worst polluting gases of the present industrial age. Until today, the key technology for preventing N_2O from mixing into the main airstream is reduction or decomposition over a suitable catalyst, which is commonly known as an "end-of-pipe" treatment.[5]

The catalysts that have been employed for the reduction of N_2O include zirconia,[6] platinum,[7,8] or α-manganese sesquioxide[9] in old times. In modern days, the catalysts that have been introduced successfully for the reduction of N_2O are the MFI type of zeolites, mainly Fe-ZSM-5, used at about 773 K in the presence of a small amount of NO_x as a promoter.[10−16] Very recently, it has been claimed that a bimetallic ferrierite (FER) catalyst containing iron and ruthenium increases the catalytic activity.[17] Despite the major progress in the technology of catalytic removal of N_2O, the main drawback of this method is that the high temperatures required in these processes greatly increase the cost of the system.[18] Moreover, in the catalytic reduction process, N_2O cannot be recovered, as it could be reutilized as an intermediate for the synthesis of some valuable fine chemicals.[19,20]

The removal of N_2O by adsorption in porous materials is uncommon as compared to the catalytic reduction strategy. Adsorption of N_2O in silicalite-1 was performed by Groen et al.[5] over the temperature range of (273 to 398) K and pressure up to 120 kPa, and the adsorption capacity of N_2O obtained was 2.5 $mol \cdot kg^{-1}$ at 273 K. The Henry's law constant and enthalpy of adsorption were also calculated to characterize the gas−solid interactions. Different varieties of activated carbon were evaluated for N_2O adsorption by Peng et al.[21] over the temperature range of (195 to 323) K and pressures up to 101 kPa. The N_2O adsorption capacities were reported to be within (12 to 18) $mol \cdot kg^{-1}$ with a typical type III isotherm for all of the activated carbon adsorbents. MOF-5, MOF-177, and zeolite 5A were employed for the adsorption of N_2O by Saha et al.[18] The highest adsorption capacity was obtained on zeolite 5A (mass fraction, $w = 0.177$), followed by MOF-5 ($w = 0.044$) and MOF-177 ($w = 0.003$) at an ambient temperature and N_2O gas pressure up to 1 bar. They also calculated the intracrystalline diffusivity of N_2O within the adsorbents, and those were reported as ($1.9 \cdot 10^{-11}$, $1.1 \cdot 10^{-9}$, and $2.2 \cdot 10^{-9}$) $m^2 \cdot s^{-1}$ for zeolite 5A, MOF-5, and MOF-177, respectively.[18] The adsorption of N_2O was also reported in certain types of pseudomorphs by Lamb and West.[22]

The objective of this study is to measure the adsorption equilibrium and kinetics of nitrous oxide on zeolite 4A and 13X. The adsorption equilibrium was measured volumetrically at three different temperatures, (194, 237, and 298) K, and kinetic data were measured at 298 K and N_2O pressure up to 108 kPa. The heat of adsorption was calculated from the adsorption isotherms at the three temperatures, which allows us to compare the adsorbate−adsorbent interaction. The diffusivity values of N_2O in the adsorbents were estimated from the kinetic data. These data will provide necessary information for the adsorbent selection and performance comparison; they will also help us to understand the adsorption fundamentals.

2. Experimental Section

The two zeolite samples (4A and 13X) were kindly provided by Mr. Li Shenan of Nanjing Refinery, SINOPEC, China.

2.1. Adsorption Experiments. The equilibrium and kinetics of nitrous oxide adsorption on both adsorbents were measured volumetrically in a Micromeritics ASAP 2020 surface area and porosity analyzer. Adsorption isotherms were measured at three temperatures, (194, 237, and 298) K, and N_2O pressures up 108 kPa. The temperature of the sample bath was constantly monitored with the help of a thermocouple, and it was observed that the temperature variation was no more than ± 1 K for experiments at 298 K and ± 2 K for experiments at (237 and 194) K, respectively. These temperatures [(194, 237, and 298) K] were achieved by using dry ice, a solid form of a commercially available engine coolant, and room temperature water, respectively. Kinetic data were recorded during the isotherm measurements at 298 K and four different pressures. The zeolite samples were activated at 623 K under a vacuum

* Corresponding author. Phone: +1 819 383 7161, e-mail: dipendus@gmail.com.

10.1021/je100105z
Published on Web 04/12/2010

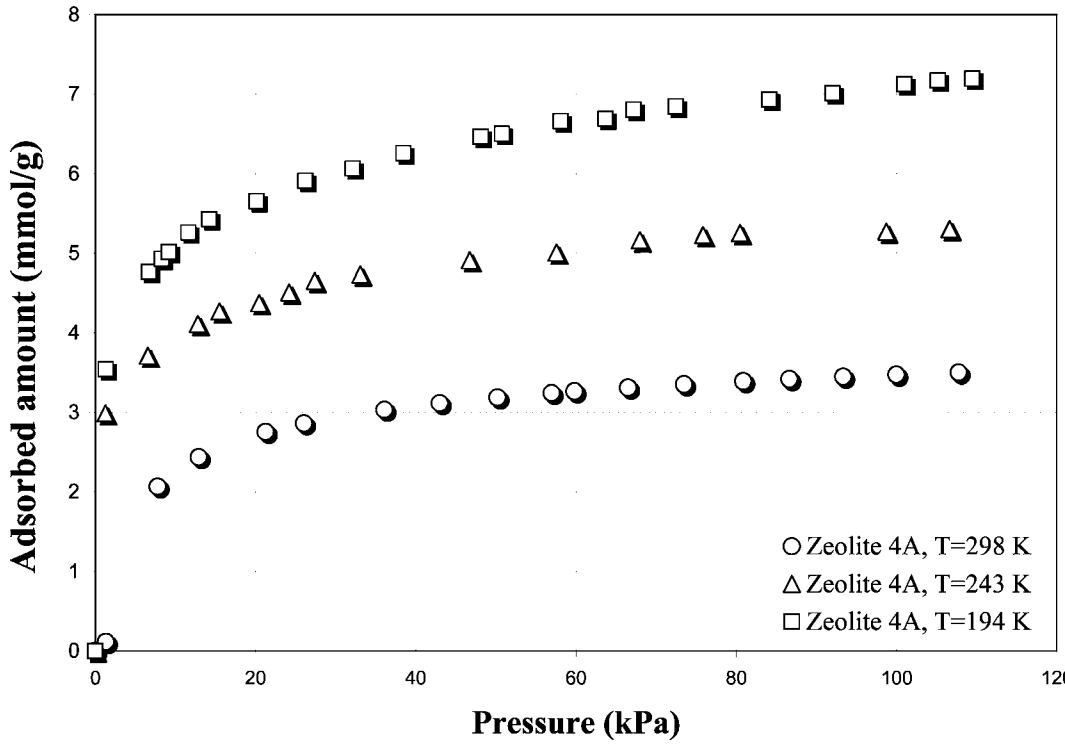

Figure 1. N_2O adsorption isotherms in zeolite 4A at (298, 237, and 194) K.

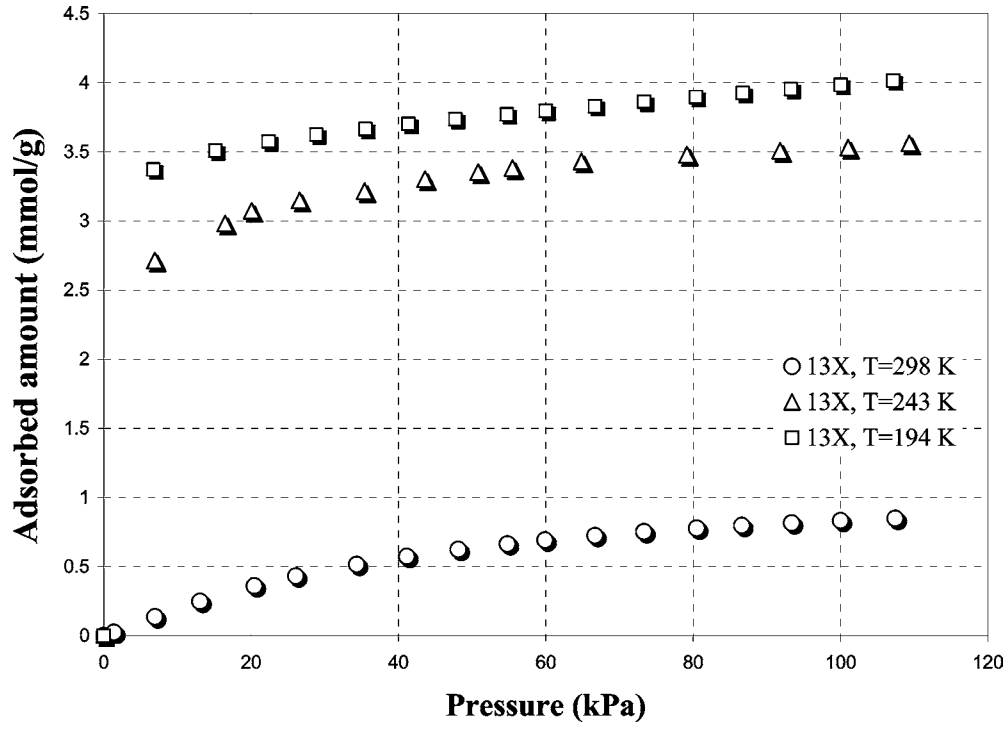

Figure 2. N_2O adsorption isotherms in 13X at (298, 237, and 194) K.

($1.33 \cdot 10^{-6}$ kPa) for 12 h before the adsorption measurements. High purity nitrous oxide (99+ %) was introduced into a gas port of the adsorption unit for the adsorption measurements. To ensure that the instrument is measuring each data point accurately, it was calibrated by employing two standards which were provided by the instrument manufacturing company, and it was found that the measured values are within ± 2 % error with the given values. Each of the isotherms reported in this paper is repeated thrice, and it was noticed that the data points vary no more than ± 1 %.

3. Results and Discussion

3.1. Adsorption Equilibrium. Adsorption isotherms of nitrous oxide on both zeolite 4A and 13X at (298, 237, and 194) K are shown in Figures 1 and 2, respectively. All of the isotherms are of type I according to the IUPAC nomenclatures. It is observed from the isotherms shown in Figures 1 and 2 that zeolite 4A adsorbs more N_2O than 13X. The adsorption amounts at (298, 237, and 194) K and a N_2O pressure of 107 kPa are (3.49, 5.3, and 7.29) $mmol \cdot g^{-1}$ for zeolite 4A, as compared to

Table 1. Isotherm Model Parameters for Zeolite 4A

isotherm model	model parameters	temperature (K)	parameter values	ARE %
Langmuir model	a_m	298	3.604	6.59
	b		0.166	
	a_m	237	4.873	28.30
	b		1.159	
	a_m	194	6.464	44.55
	b		0.829	
Freundlich model	k	298	0.274	61.83
	n		1.630	
	k	237	2.930	4.45
	n		7.541	
	k	194	3.534	5.39
	n		6.476	
Toth model	k_T	298	0.434	19.08
	α_T		399.468	
	t		0.060	
	k_T	237	0.163	4.43
	α_T		399.49	
	t		0.030	
	k_T	194	0.199	3.32
	α_T		399.42	
	t		0.038	

Table 2. Isotherm Model Parameters for 13X

isotherm model	model parameters	temperature (K)	parameter values	ARE %
Langmuir model	a_m	298	4.304	13.03
	b		0.003	
	a_m	237	3.517	6.19
	b		0.433	
	a_m	194	3.900	7.56
	b		0.782	
Freundlich model	k	298	0.026	6.98
	n		1.259	
	k	237	2.275	1.76
	n		10.298	
	k	194	2.945	2.35
	n		15.772	
Toth model	k_T	298	1.984	2.55
	α_T		136.84	
	t		0.140	
	k_T	237	0.115	1.63
	α_T		134.334	
	t		0.0256	
	k_T	194	0.073	2.27
	α_T		134.35	
	t		0.018	

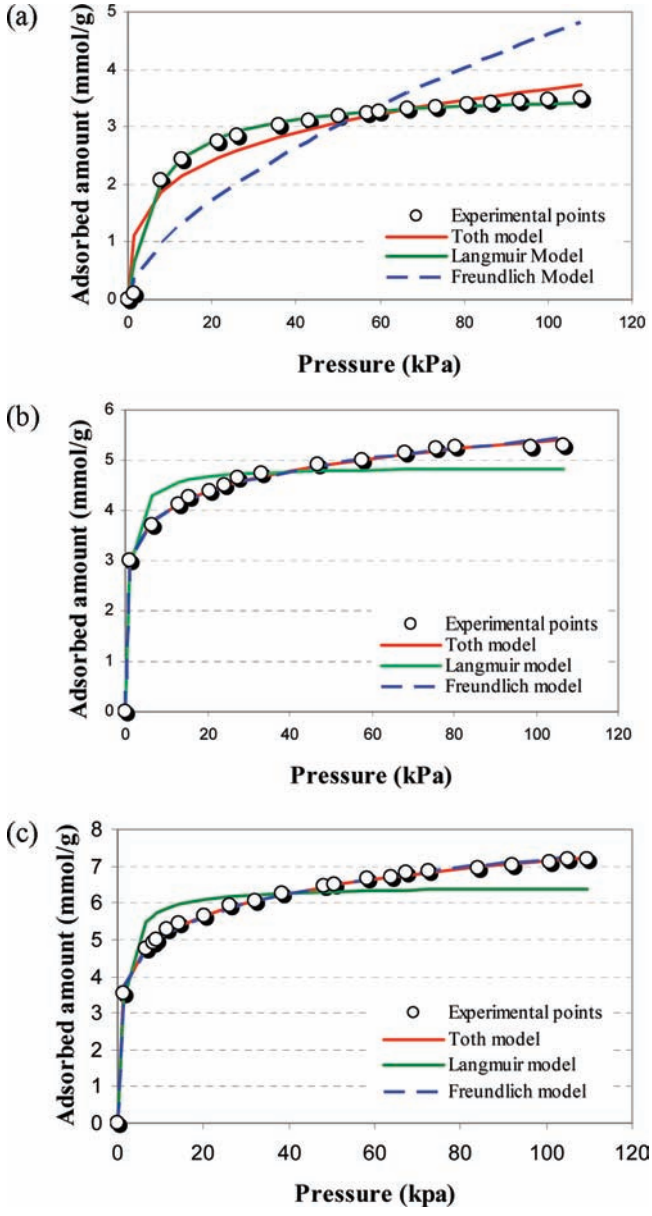

Figure 3. Comparison isotherm model parameters for zeolite 4A at 298 K (a), 237 K (b), and 194 K (c).

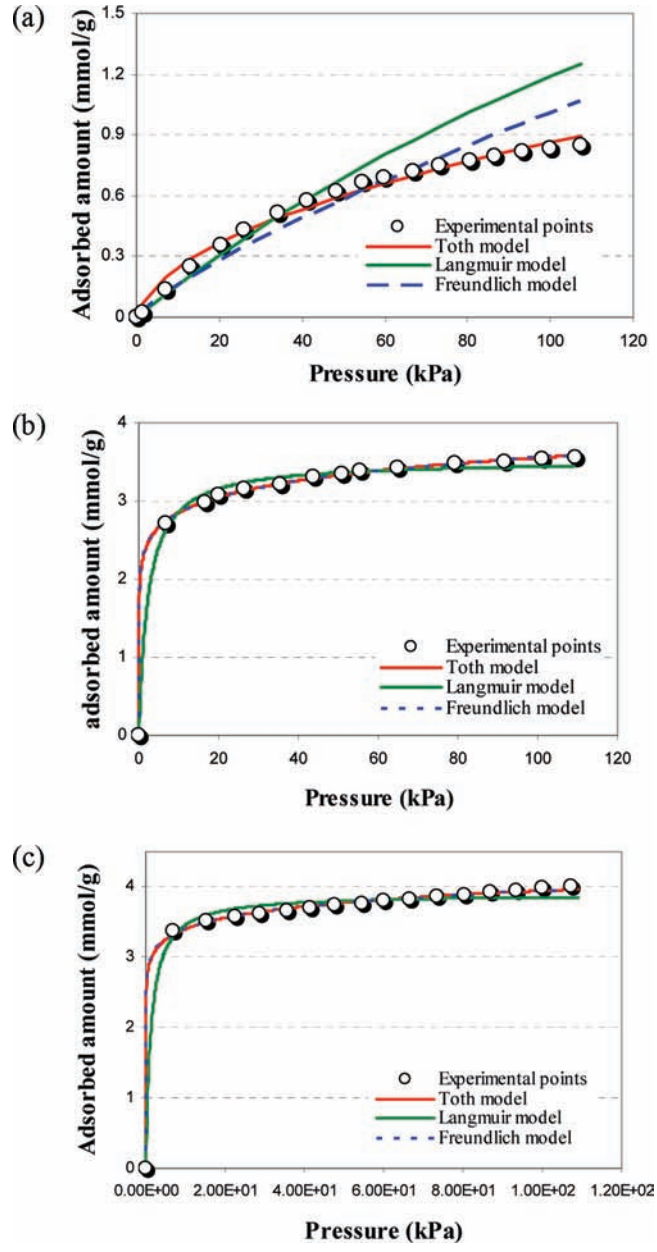

Figure 4. Comparison isotherm model parameters for 13X at 298 K (a), 237 K (b), and 194 K (c).

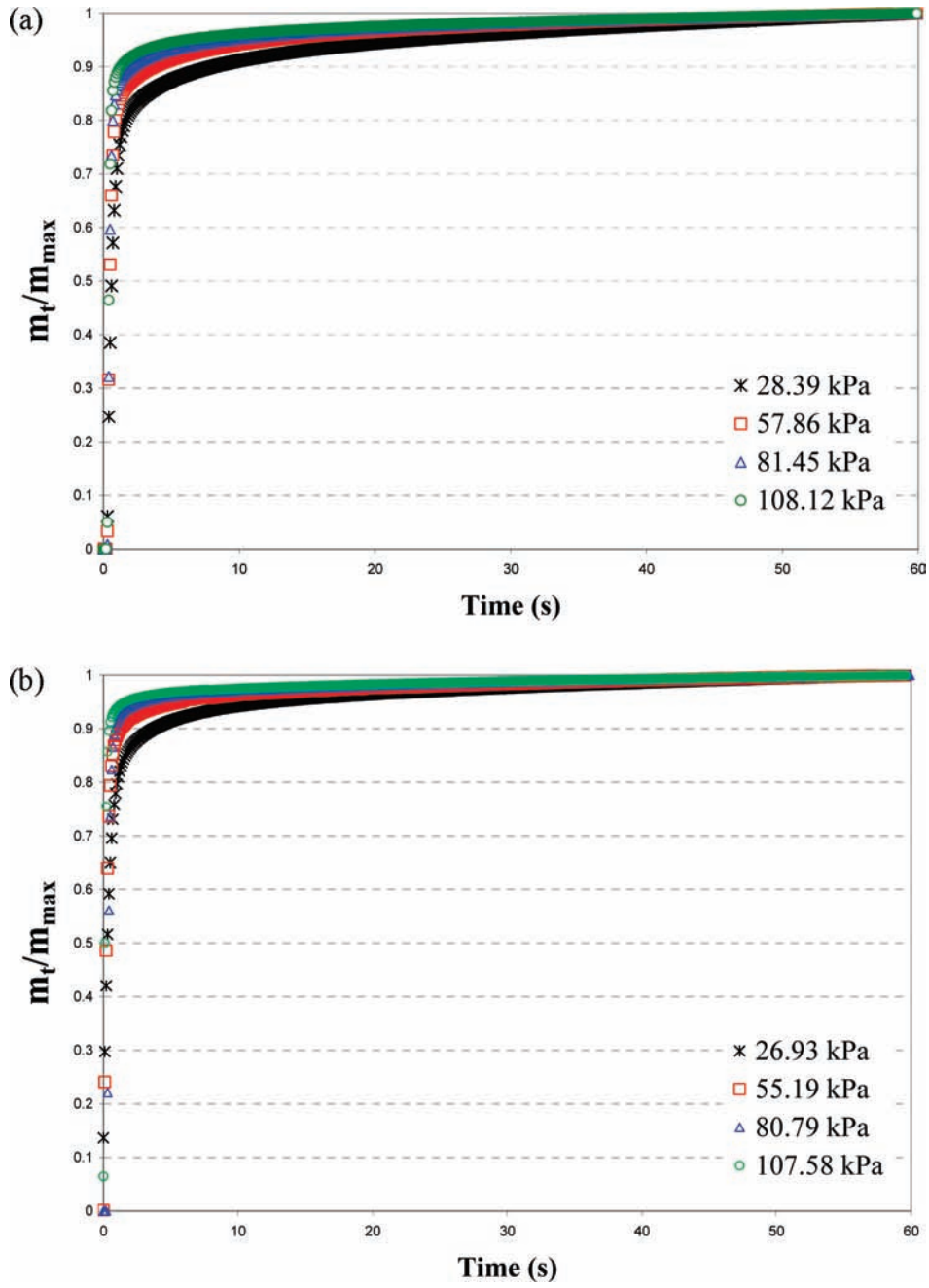

Figure 5. Kinetic plots of N_2O adsorption on to zeolite 4A (a) and 13X (b).

(0.84, 3.58, and 3.96) mmol·g^{-1} for 13X. The N_2O adsorption capacity at 298 K and N_2O pressure about 1 bar on 4A is higher than that of silicalite-1 (around 1.75 mmol·g^{-1}) reported by Groen et al.[5] but lower than that of zeolite 5A (4.03 mmol·g^{-1}) reported by Saha et al.[18] However, the N_2O uptake by both zeolite 4A and 13X is significantly higher than that of the metal−organic framework MOF-5 (1 mmol·g^{-1}) and MOF-177 (0.07 mmol·g^{-1}) at similar conditions.[18] The highest adsorption amount at the terminal pressure measured in this work is lower than the values on activated carbon reported by Peng et al.,[21] but because of the typical type-III nature of their isotherms, the adsorption amount seems to be greater on zeolites 4A and 13X at the lower pressure range.

The adsorption isotherms obtained in this work were correlated with the Langmuir, Freundlich, and Toth isotherm equations. The Langmuir equation is given by

$$q = \frac{a_m bp}{1 + bp} \tag{1}$$

where a_m (mmol·g^{-1}) is the monolayer adsorption capacity and b (kPa^{-1}) is the Langmuir adsorption equilibrium constant. Both parameters can be determined from the slope and intercept of a linear plot of $1/p$ versus $1/q$.

The Freundlich model can be written as

$$q = kp^{1/n} \tag{2}$$

where k and n are the equation model parameters which can be calculated from a linear plot of ln p versus ln q.

The Toth model can be given by

$$q = \frac{\alpha_T p}{(k_T + p^t)^{1/t}} \tag{3}$$

where α_T, k_T, and t are equation constants which can be

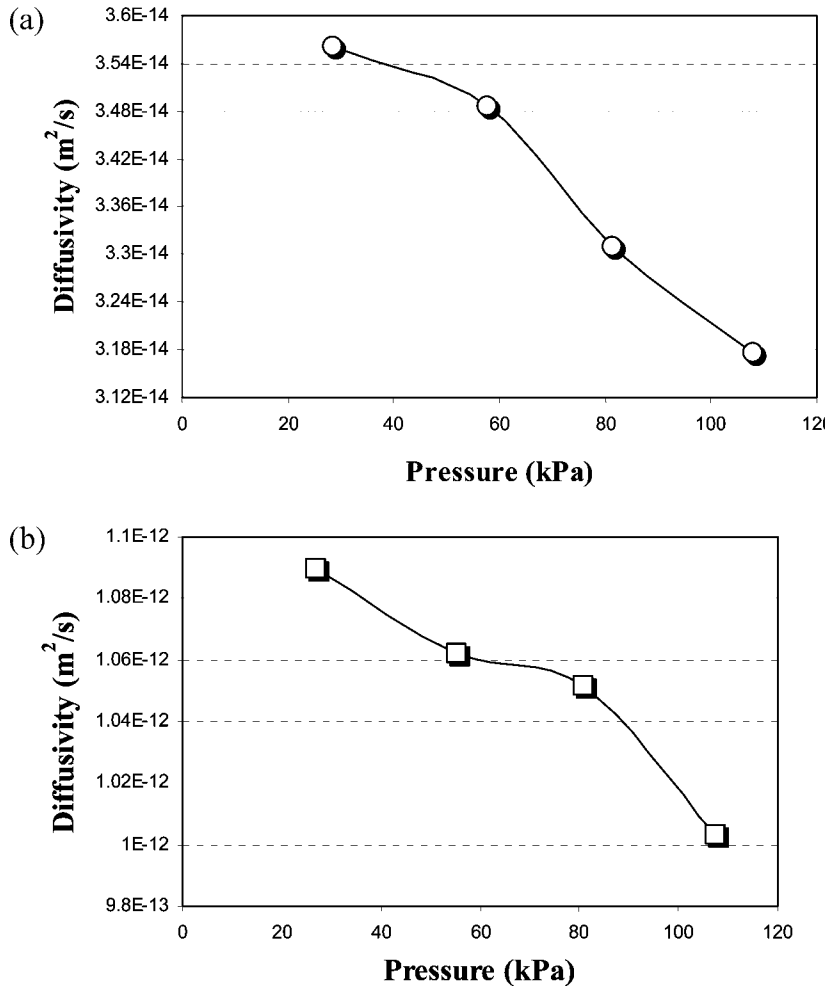

Figure 6. Variation of N_2O diffusivity with pressure for zeolite 4A (a) and 13X (b).

determined by nonlinear regressions. The degree of model fitting was compared by the absolute relative error (ARE) percent, calculated as

$$\text{ARE \%} = \frac{\sum_{n=1}^{N} |x_{exp} - x_{mod}|}{N} \cdot 100\ \% \qquad (4)$$

where x_{exp} is the experimental point, x_{mod} is the modeling point, and N is the number of points in the isotherm.

Tables 1 and 2 summarize the isotherm model parameters and ARE values for zeolite 4A and 13X, respectively. Figures 3a−c and 4a−c compare the model fitting with the experimental values for zeolite 4A and 13X at (298, 237, and 194) K, respectively. From the tables, it is found that the Langmuir model fits better at 298 K for zeolite 4A; however, the Toth model seems to be better for the remaining isotherms on zeolite 4A. For 13X, the Toth model fits the best for all three isotherms.

3.2. Adsorption Kinetics. Adsorption kinetic data of nitrous oxide were collected at the same time, when the isotherms were generated at 298 K and pressure up to 108 kPa. Figure 5a,b shows the kinetic plots at four different pressure ranges for zeolite 4A and 13X, respectively. It is observed that zeolite 4A and 13X reached the adsorption saturation level within (50 to 60) s and (40 to 50) s, respectively. A classical micropore diffusion model was applied to analyze the kinetic data and to estimate the diffusivity of nitrous oxide in the zeolites. For fractional uptakes (m_t/m_∞) higher than 70 %, the diffusion model equation can be written as,[23]

$$1 - \frac{m_t}{m_\infty} = \frac{6}{\pi^2} \exp\left(\frac{-\pi^2 D_c t}{r_c^{\,2}}\right) \qquad (5)$$

where D_c is the intracrystalline diffusivity, r_c is the equivalent crystal radius, and t is time. The diffusion time constants ($D_c/r_c^{\,2}$) and s^{-1} were calculated from the slope of a linear plot of $\ln(1 - (m_t/m_\infty))$ versus t at a given N_2O pressure. It has been found from the scanning electron microscopy images that the zeolite 4A and 13X samples possess the equivalent crystalline radius of ($2.5 \cdot 10^{-6}$ and $2.54 \cdot 10^{-5}$) m, respectively. From these crystal radius size values, the average diffusivity of N_2O in zeolite 4A and 13X is calculated to be ($3.38 \cdot 10^{-14}$ and $1.05 \cdot 10^{-12}$) $m^2 \cdot s^{-1}$, respectively. Both of these values are lower than that of zeolite 5A, MOF-5, and MOF-177, reported by Saha et al.[18] It is quite challenging to explain the difference between the diffusivity values within these zeolite samples, but most probably, the smaller pore opening of zeolite 4A is responsible for the slower kinetics as compared with 13X. The variations of diffusivity with pressure are shown in Figure 6a,b for zeolite 4A and 13X. It is observed that the diffusivity values decrease with the increase in pressure. This trend is probably attributed to the fact that the pores of the zeolites materials were partially saturated and blocked at the higher adsorption loading at higher pressures.

3.3. Isosteric Heat of Adsorption. The isosteric heat of adsorption values are a quite important parameter revealing the adsorbate−adsorbent interactions. Isosteric heat of adsorption can be calculated from the van't Hoff equation:

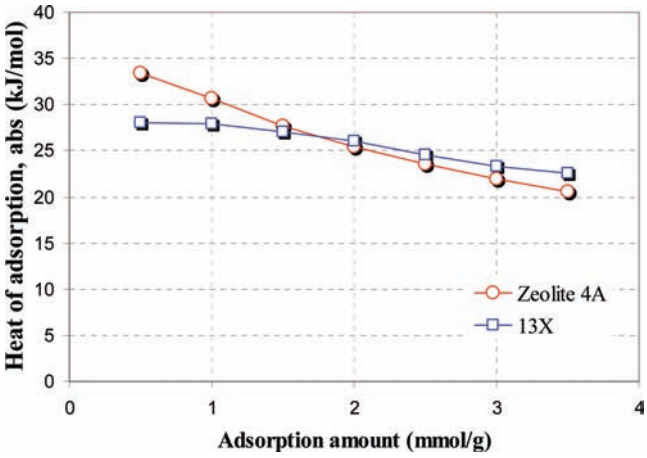

Figure 7. Heat of N_2O adsorption for zeolite 4A and 13X.

$$\frac{\Delta H}{RT^2} = -\left(\frac{\partial \ln P}{\partial T}\right)_a \quad (6)$$

where ΔH is the isosteric heat of adsorption ($kJ \cdot mol^{-1}$), P is gas pressure (kPa), T is temperature, and a is the adsorption amount ($mmol \cdot g^{-1}$). The integration of eq 6 yields:

$$\ln P = \frac{\Delta H}{RT} + C \quad (7)$$

where C is an integration constant. In this work, the isotherms at (194, 237, and 298) K were employed to calculate the heat of adsorption values. The isotherm data points were first converted to a set of isosters (linear plot of ln P versus $1/T$) and then correlated with eq 7, and the heat of adsorption was then calculated from the slope of the isosters according to eq 7. The variation of heat of adsorption with adsorption loadings is then plotted in Figure 7. It is observed that these values were almost in the same range for both kinds of materials, (−33 to −21) $kJ \cdot mol^{-1}$ for zeolite 4A and (−28 to −22) $kJ \cdot mol^{-1}$ for 13X within the adsorption loading of (0.5 to 3.5) $mmol \cdot g^{-1}$, suggesting that N_2O interacts with the two zeolites similarly.

4. Conclusions

It is observed that zeolite 4A adsorbs N_2O more than the 13X sample at (194, 237, and 298) K and N_2O pressures up to 108 kPa. The highest N_2O uptake on 4A, 7.2 $mmol \cdot g^{-1}$, as compared with 4 $mmol \cdot g^{-1}$ on 13X was obtained at 194 K and 108 kPa. All of the isotherms were modeled by Langmuir, Freundlich, and Toth models, and it was found that the Toth model fits the best for most of the isotherms. A kinetic study reveals that the average diffusivity of N_2O in zeolite 4A and 13X was ($3.38 \cdot 10^{-14}$ and $1.05 \cdot 10^{-12}$) $m^2 \cdot s^{-1}$, respectively. The slower kinetics in zeolite 4A is probably caused by its narrower pore opening. The diffusivity values decrease with N_2O pressure for both zeolites, which is probably caused by the partial pore blocking at the greater adsorption amount at higher pressures. The heat of adsorption values were calculated to be (−33 to −21) $kJ \cdot mol^{-1}$ for zeolite 4A and (−28 to −22) $kJ \cdot mol^{-1}$ for 13X within the adsorption loading of (0.5 to 3.5) $mmol \cdot g^{-1}$. The similar heat of adsorption values suggest that N_2O interacts with both zeolites similarly.

Literature Cited

(1) Rodhe, H. A. comparison of the contribution of various gases to the greenhouse effect. *Science* **1990**, *248*, 1217–1219.
(2) Theimens, M. H.; Trogler, W. C. Nylon Production: An Unknown Source of Atmospheric Nitrous Oxide. *Science* **1991**, *251*, 932.
(3) Centi, G.; Perathoner, S.; Vanazza, F. Catalytic control of non-CO_2 greenhouse gases. *CHEMTECH* **1999**, *12*, 48–55.
(4) Kapteijn, F.; Rodríguez-Mirasol, J.; Moulijn, J. A. Heterogeneous catalytic decomposition of nitrous oxide. *Appl. Catal., B* **1996**, *9*, 25–64.
(5) Groen, J. C.; Ramírez, J. P.; Zhu, W. Adsorption of Nitrous Oxide on Silicalite-1. *J. Chem. Eng. Data* **2002**, *47*, 587–589.
(6) Miller, T. M.; Grassian, V. H. Environmental Catalysis: Adsorption and Decomposition of Nitrous Oxide on Zirconia. *J. Am. Chem. Soc.* **1995**, *117*, 10969–10975.
(7) Redmoxd, J. P. Kinetics of the low pressure nitrous oxide decomposition on a platinum filament. *J. Phys. Chem.* **1963**, *67*, 788–793.
(8) Watanabe, K.; Kokalj, A.; Inokuchi, Y.; Rzeznicka, I.; Ohshimo, K.; Nishi, N.; Matsushima, T. Orientation of nitrous oxide on palladium (1 1 0) by STM. *Chem. Phys. Lett.* **2005**, *406*, 474–478.
(9) Rheaume, L.; Parravano, G. Decomposition kinetics of nitrous oxide on α-manganese sesquioxide. *J. Phys. Chem.* **1959**, *63*, 264–268.
(10) Kogel, M.; Abu-Zied, B. M.; Schwefer, M.; Turek, T. The effect of NO_x on the catalytic decomposition of nitrous oxide over Fe-MFI zeolites. *Catal. Commun.* **2001**, *2*, 273–276.
(11) Perez-Ramirez, J.; Kapteijn, F.; Mul, G.; Moulijn, J. A. Superior performance of ex-framework FeZSM-5 in direct N_2O decomposition in tail-gases from nitric acid plants. *Chem. Commun.* **2001**, 693–694.
(12) Perez-Ramirez, J.; Kapteijn, F.; Mul, G.; Moulijn, J. A. Highly active SO_2-resistant ex-framework FeMFI catalysts for direct N_2O decomposition. *Appl. Catal., B* **2002**, *35*, 227–232.
(13) Guzman-Vargas, A.; Delahay, G.; Coq, B. Catalytic decomposition of N_2O and catalytic reduction of N_2O and N_2O + NO by NH_3 in the presence of O_2 over Fe-zeolite. *Appl. Catal., B* **2003**, *42*, 369–379.
(14) Pieterse, J. A. Z.; Booneveld, S.; van den Brink, R. W. Evaluation of Fe-zeolite catalysts prepared by different methods for the decomposition of N_2O. *Appl. Catal., B* **2004**, *51*, 215–228.
(15) Sobolev, V. I.; Panov, G. I.; Kharitonov, A. S.; Romannikov, V. N.; Volodin, A. M.; Ione, K. G. Catalytic Properties of ZSM-5 Zeolites in N_2O Decomposition: The Role of Iron. *J. Catal.* **1993**, *139*, 435–443.
(16) Panov, G. I.; Uriarte, A. K.; Rodkin, M. A.; Sobolev, V. I. Generation of active oxygen species on solid surfaces. Opportunity for novel oxidation technologies over zeolites. *Catal. Today* **1998**, *41*, 365–385.
(17) Pieterse, J. A. Z.; Mul, G.; Melian-Cabrera, I.; van den Brink, R. W. Synergy between metals in bimetallic zeolite supported catalyst for NO-promoted N_2O decomposition. *Catal. Lett.* **2005**, *99*, 41–44.
(18) Saha, D.; Bao, Z.; Jia, F.; Deng, S. Adsorption of CO_2, CH_4, N_2O and N_2 on MOF-5, MOF-177 and zeolite 5A. *Environ. Sci. Technol.* **2010**, *44*, 1820–1826.
(19) Panov, G. I. Advances in oxidation catalysis; oxidation of benzene to phenol by nitrous oxide. *CATTECH* **2000**, *4*, 18–31.
(20) Hoelderich, W. Environmentally benign manufacturing of fine and intermediate chemicals. *Catal. Today* **2000**, *62*, 115–130.
(21) Peng, Y.; Zhang, F.; Xu, C.; Xiao, Q.; Zhong, Y.; Zhu, W. Adsorption of nitrous oxide on activated carbons. *J. Chem. Eng. Data* **2009**, *54*, 3079–3081.
(22) Lamb, A. B.; West, C. D. The Adsorption of Nitrous Oxide on Certain Pseudomorphs. *J. Am. Chem. Soc.* **1940**, *62*, 3176–3180.
(23) Ruthven, D. M. *Principles and adsorption and adsorption processes*; Wiley Interscience: New York, 1984.

Received for review January 29, 2010. Accepted April 03, 2010.

JE100105Z